

## **UC Davis**

### **UC Davis Previously Published Works**

#### **Title**

Fingerprinting Inhomogeneities in Recording Media Using the First-Order Reversal Curve Method

#### **Permalink**

<https://escholarship.org/uc/item/0571f3g1>

#### **Journal**

IEEE TRANSACTIONS ON MAGNETICS, 47(10)

#### **Authors**

Valcu, Bogdan F.  
Gilbert, Dustin A.  
Liu, Kai

#### **Publication Date**

2011-09-23

Peer reviewed

# Fingerprinting Inhomogeneities in Recording Media Using the First-Order Reversal Curve Method

Bogdan F. Valcu<sup>1</sup>, Dustin A. Gilbert<sup>2</sup>, and Kai Liu<sup>2</sup>

<sup>1</sup>Seagate Technology, Fremont, CA 94538 USA

<sup>2</sup>Physics Department, University of California Davis, Davis, CA 95616 USA

Understanding how interactions within magnetic systems affect the reversal process is critical to the development of magnetic recording media. Using the first-order reversal curve (FORC) method we demonstrate an ability to map out and uniquely identify magnetic recording media. We evaluate the interactions and intrinsic switching field distribution (SFD) in single layer and exchange coupled composite granular recording media. Landau–Lifshitz–Gilbert-based simulations are used to probe the roles lateral and vertical exchange interactions have on the distribution of reversal events. We find that there is an optimal value for these terms which maximizes homogeneity of the reversal behavior.

**Index Terms**—Composite media, first-order reversal curve (FORC), inhomogeneities, micromagnetics.

## I. INTRODUCTION

AS perpendicular magnetic recording reaches maturity it has become apparent that, due to the limitations of the magnetic properties of CoCrPt-based granular films, the reduction of grain size is very challenging; consequently advances in areal density are driven more by a better control of the switching field distribution (SFD) of the media. SFD is typically evaluated by magnetometry measurements, such as vibrating sample magnetometry or magneto-optical Kerr effect (MOKE), where the entire sample is subject to a magnetic field. Switching of a particular grain depends on both its intrinsic anisotropy and its interactions with neighboring grains. The interaction fields during such measurement are different from those experienced by grains during recording under a local magnetic field. Thus, it is imperative to separate the interactions from the switching field, namely to obtain an intrinsic SFD. The method proposed by Berger *et al.* [1] uses a collection of minor loops, in addition to the major loop, to address this very issue: the differences between each minor loop and the major loop at various constant magnetization  $M$  values are calculated and the interaction field is eliminated. The distribution of the grains' switching fields in the absence of interactions is obtained [2], and can be used to optimize recording media [3].

First-order reversal curve (FORC) analysis presents an alternative method to evaluate the intrinsic properties of the sample, as well as the intrasample interactions. The FORC method is a mathematical process based on the Preisach model, which uses a family of partial hysteresis loops to characterize switching events in hysteretic systems [4]–[9]. It can reveal more information than a traditional 1-D SFD: it maps out the distribution of switching events in terms of the coercivity distribution and the interaction fields. This makes it particularly useful to fingerprint the switching events in recording media.

This characterization has become more relevant as magnetic recording media have become more complex. In recent years

recording media design migrated from a recording stack consisting of a single layer of magnetic grains isolated by nonmagnetic grain boundaries, to a multilayer stack, with one or more granular layers at the bottom covered by a continuous layer at the top [10]. The layers have different anisotropy field ( $H_k$ ) values, as well as different intergranular exchange values. This is done in order to reduce the switching field while maintaining thermal stability [11], [12]. The reversal mechanism in these multilayer films differs from the Stoner–Wohlfarth model, and proceeds through incoherent rotation of magnetization in the various layers (exchange coupled composite media effect [13], or vertical domain wall motion reversal [14]).

In this work, we report on the large qualitative differences between the measured FORC distributions of various types of recording media. To deconstruct these diagrams we use micromagnetics to simulate the minor and major loops of multilayer structures in which magnetic properties are varied in a controlled way. In Section II, we review the literature that presents the FORC diagrams in light of the interacting hysterons model. Section III describes how we measured the experimental FORC distributions for various recording media designs. Section IV briefly describes first our micromagnetic model. Then, we use the FORC distributions modeled for a set of varying micromagnetic parameters to explain the features of the experimental FORCs. Section V concludes the paper.

## II. THE FORC METHOD

The FORC method can capture the distribution of irreversible switching events in a hysteretic system. A FORC distribution is experimentally derived by first collecting a family of minor loops that always start from positive saturation. These minor loops can be seen as a 2-D map of magnetization  $M(H_a, H_r)$  (see Fig. 1), where  $H_a$  is the applied field and  $H_r$  is the return field along each minor loop. The ascending branch of each minor loop, known as a first-order reversal curve, is then extracted. We then apply a mixed second-order derivative to the magnetization with respect to  $H_a$  and  $H_r$ , and develop the FORC distribution

$$\rho(H_a, H_r) = -\frac{1}{2} \frac{\partial^2 M(H_a, H_r)}{\partial H_a \partial H_r}. \quad (1)$$

Manuscript received February 21, 2011; accepted April 11, 2011. Date of current version September 23, 2011. Corresponding author: B. F. Valcu (e-mail: bvalcu@hotmail.com).

Color versions of one or more of the figures in this paper are available online at <http://ieeexplore.ieee.org>.

Digital Object Identifier 10.1109/TMAG.2011.2146241

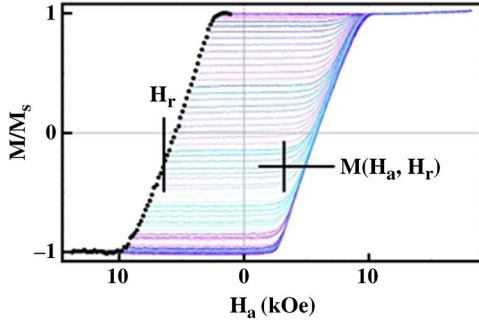


Fig. 1. Family of FORCs for a simulated two-layer recording media stack.

The FORC distribution maps the hysteretic reversal events in terms of their reversal field and saturation field. It does this by expanding the physical hysteresis loop into a weighted sum of elemental square hysteresis loops called hysterons [7]. Each hysteron has a unit magnetization ( $\pm 1$ ), with a well-defined reversal field (“switch-down” field  $H_r$ ) and saturation field (“switch-up” field  $H_a$ ); the FORC distribution maps the weight function for the hysterons. For a single hysteron the FORC distribution is the product of two delta Dirac functions:  $\delta(H_r)\delta(H_a)$ . The coordinate space spanning the reversal and saturation fields does not describe the intrinsic properties of the sample. Using a simple transformation

$$H_b = (H_a + H_r)/2, \quad H_c = (H_a - H_r)/2 \quad (2)$$

the FORC distribution can instead map the reversal events in terms of a bias field  $H_b$  and local coercivity  $H_c$ . The local coercivity describes the intrinsic properties of the system, while the bias axis generally describes the interaction fields.

Elementary FORC distributions were modeled in [7] and [15] for an ensemble of hysterons which experience an interaction field in addition to the applied field. The loops are simulated as follows. Initially, all the hysterons have a magnetization equal to  $+1$ ; subsequently, the field is decreased in small steps, and the interaction field for each hysteron is calculated. If the applied field plus the interaction field is larger than the coercivity of a hysteron, that hysteron changes magnetization to  $-1$ . The field is decreased to the next step and iteration proceeds [7].

If the interaction field is equal to  $(-\alpha \cdot M)$ , where  $M$  is the average magnetization and  $\alpha$  is a constant, and all hysterons have the same coercivity  $H_c$ , then the FORC distribution is a narrow vertical band parallel to the  $H_b$  axis, extending from  $H_b = -\alpha$  to  $+\alpha$  at  $H_c$ . (This has been experimentally observed in arrays of magnetic nanowires where the interaction field is dipolar [16].) If there is no interaction field but a distribution in the coercivities of the hysterons, then the FORC diagram is a narrow horizontal band parallel to the  $H_c$  axis at  $H_b = 0$ . This would represent the intrinsic SFD. Finally, if there are both interactions and an  $H_c$  distribution, a wishbone shape is generated, as seen in [7]. The upper branch of the wishbone has a strong peak at the intercept with the vertical branch. Similar FORC diagrams are also generated in [15].

### III. EXPERIMENTAL FORC

We have measured families of FORCs using a fast MOKE. The applied field is swept from positive maximum to negative minimum in approximately 1 s, with field amplitude of around

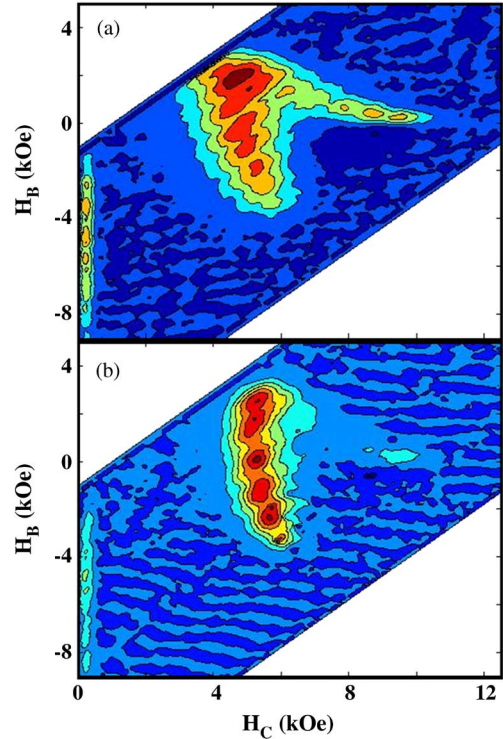


Fig. 2. (a) FORC distribution from single-layer magnetic recording media similar to those developed in the early days of perpendicular recording, which exhibits the well-understood “wishbone” structure. (b) FORC distribution for a multilayer magnetic recording media more closely related to modern recording media. The tail of the “wishbone” structure is largely suppressed as a result of the multilayer coupling.

2 Tesla. The MOKE is limited by the penetration depth of the probing laser, thus magnetometry data reflect only the recording stack. After acquisition the loops are resampled so that the field step is constant, 200 Oe. To calculate the FORC distribution we use the technique described in [5]: seven consecutive minor loops are used at a time to fit  $M(H_a, H_r)$  to a third-order polynomial. Once the polynomial coefficients are known, the second derivative needed for the FORC distribution (1) is easily calculated. The function  $\rho(H_c, H_b)$  is shown as a colored surface plot; contours are added for a more quantitative description. Typically, we acquire 75 minor loops for each family of FORCs, so that we have a small enough step in  $H_r$ . This ensures a high resolution for the maps. Following these methods we have evaluated the FORC distribution for two examples of recording media.

Fig. 2(a) presents the experimentally determined FORC distribution for a medium used in the early days of perpendicular recording. The recording stack comprised only a single granular layer. The FORC distribution illustrates the wishbone shape, with the vertical band positioned at  $H_c = 5$  kOe, and a strong peak at  $H_b = 2$  kOe. The interaction field in perpendicular media encourages antiparallel alignment between neighboring grains, defining a demagnetizing interaction. Together with the distribution in the grains switching fields ( $H_c$  distribution), the demagnetizing interactions generate the wishbone structure described in the hysteron model.

Very interestingly, the measured diagram for the newer media design [Fig. 2(b)], which structurally has many layers of various  $H_k$  values, has a much less pronounced wishbone shape,

approaching essentially a narrow vertical band shape. This vertical band has the higher peak at negative value of the interaction field  $H_b = -3$  kOe, as opposed to that at  $H_b = 2$  kOe in Fig. 2(a); this experimental fact cannot be explained by the hysteron model.

The differences between the FORC distributions of these two media are apparent; the FORC distribution has allowed us to uniquely fingerprint each of our recording media and extract useful information about the reversal process.

#### IV. MICROMAGNETIC MODEL AND FORC DISTRIBUTIONS

To simulate the hysteresis loops of the multilayer recording media we have employed standard micromagnetics [17]. In our model, the medium is divided into many layers, to which we assign measured magnetic properties (anisotropy  $K_u$ , saturation magnetization  $M_s$ ). There are 6000 grains per layer, and each grain is divided further into many subgrains. The vertical coupling between layers is controlled by the parameter  $J$ , expressed as a fraction of the bulk exchange. The intergranular exchange  $H_{ex}$  may have different values in the various layers, to mimic the difference between the granular and continuous layers.

Hysteresis loops are calculated in the usual way: for each value of the field  $H$  the magnetization of each grain precesses until equilibrium is reached in a total effective field comprising the applied field, anisotropy field, exchange field, and a magnetostatic dipolar interaction field

$$\vec{H}_{\text{eff}} = \vec{H}_a + H_K(\vec{k} \cdot \vec{m})\vec{k} + \frac{2A^*}{D^2 M_s} \sum_{\langle nn' \rangle} \vec{m}' + M_s \sum_{\vec{r}''} \vec{D}(\vec{r} - \vec{r}'') \vec{m}(\vec{r}''). \quad (3)$$

Here  $\vec{m}$  indicates the magnetization of the grain of interest, while  $\vec{m}'$  are the magnetizations of the neighbor grains.  $\vec{D}$  is the demagnetizing tensor [18]. The intergranular exchange constant  $A^*$ , between neighbor grains in the same vertical layer, is a fraction of the bulk exchange constant  $A = 10^{-6}$  erg/cm, due to the presence of the nonmagnetic boundaries. We introduce a film-averaged exchange field as

$$H_{\text{ex}} = \left\langle 2 \left( \frac{A}{D^2} \right) \frac{1}{M_s} \right\rangle \quad (4)$$

and use  $H_{\text{ex}}$  as an input parameter in micromagnetics. The exchange interaction between neighbor grains in two adjacent vertical layers, across an exchange break layer, has a similar expression. The scaling factor  $2A^*/D^2$  is in this case replaced by  $J_{\text{surface}}/\text{thickness}$ , where  $J_{\text{surface}}$  is measured in erg/cm<sup>2</sup>, and the thickness characterizes the layer of interest. We introduce a 1-D parameter  $J$ , with  $0 < J < 1$ , to reflect how strongly the exchange interaction is reduced from the bulk value, due to the presence of the vertical break layer.

Dynamics follows the Landau–Lifshitz–Gilbert equation. No thermal fluctuations are considered (these are  $T = 0$  K or short-time loops).

The sample has a large number of grains, and the computation is very time consuming, even when computer clusters are used. We are able to accelerate our simulation significantly by running it on the graphical processing unit, rather than on the computer's central processing unit (CPU). This allowed the simulation of 75 FORC branches per sample, giving good resolution.

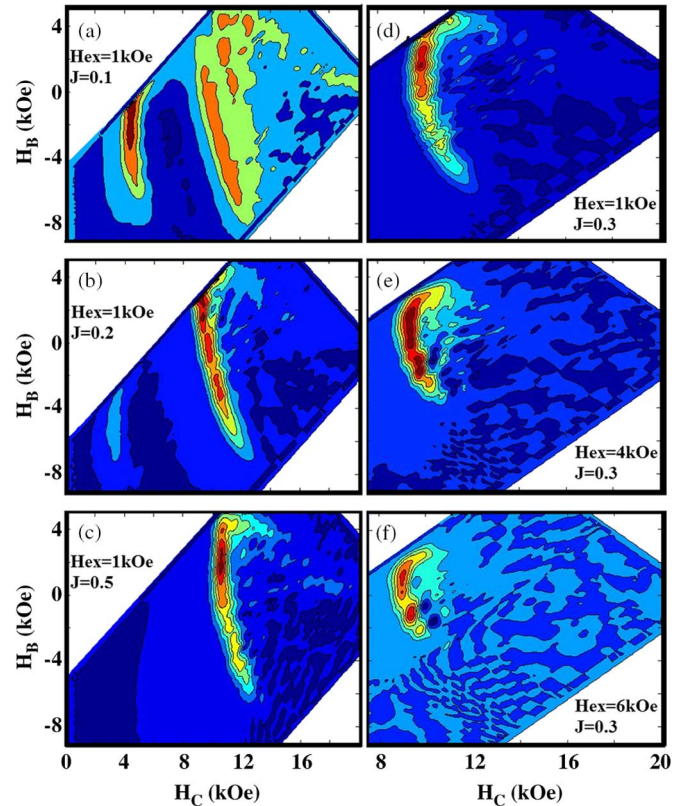


Fig. 3. Simulated FORC distributions for two-layer perpendicular recording media with lateral granular exchange ( $H_{\text{ex}}$ ) of 1 kOe, and vertical exchange coupling ( $J$ ) of (a) 0.1 (b) 0.2, and (c) 0.5. The effect of lateral intergranular exchange coupling is studied by fixing the vertical coupling constant at  $J = 0.3$  and vary  $H_{\text{ex}}$  to (d) 1 kOe, (e) 4 kOe, and (f) 6 kOe. For the weak vertical coupling (a) we see the two phases reverse separately, but for the case of larger coupling they reverse together, and the coupling manifests in the homogeneity of the ridge. For the weak lateral coupling the distribution has a well defined peak offset in the positive  $H_b$  direction. As the lateral coupling increases the feature becomes more homogeneous, then breaks again into discrete peaks.

We present here results for a media that has two layers, where each layer has a different anisotropy. To simplify the physics, we assumed that the intergranular exchange ( $H_{\text{ex}}$ ) has the same value in both layers.

##### A. Effect of Vertical Exchange Coupling $J$

In a first simulation, we keep  $H_{\text{ex}}$  at a low value, 1 kOe: both layers are granular, with well-separated grains. The bottom layer has a high anisotropy value, while the top layer has significantly lower anisotropy. These designs explore the exchange coupled composite media concept: the grain in the softer layer will switch first, pulling down the moments of the grains in the hard layer; the resulting overall switching field is significantly lower than what the average anisotropy would indicate [13]. We control the reversal of the magnetization by varying the vertical coupling  $J$  between the hard and soft layers. If the coupling is low [ $J = 0.1$ , Fig. 3(a)] the grains in the soft layer will reverse almost completely before the grains in the hard layer start to switch. Thus, the FORC diagrams consists of two distinct “islands,” one at low coercivity  $H_c = 4$  kOe corresponding to the soft layer, and the other at high coercivity  $H_c = 12$  kOe. Very interestingly, the distribution corresponding to the soft layer (left side) has *negative* values for the bias field  $H_b$ : since the grains

in the hard layer point up while the grains in the soft layer attempt to switch, the field needed for reversal is higher, thus the bias field is negative. This peak in the distribution function at  $H_b < 0$  helps us understand the origin of the strong peak at  $H_b < 0$  in the experimental FORC distribution [Fig. 2(b)]: its presence is due to the soft-on-hard media composition.

As the vertical coupling is increased to  $J = 0.2$  [Fig. 3(b)] the two islands merge together, and the resulting vertical band at  $H_c = 10$  kOe has a ridge-like structure, with a significant number of switching events at negative interaction field values (e.g.,  $H_b = -3$  kOe). This pattern closely resembles that seen in bilayer exchange spring magnet films of FeNi/FePt [19].

Further, increasing  $J$  to 0.5 [Fig. 3(c)] leads to the disappearance of the switching events at negative  $H_b$ : the FORC diagram migrates to the wishbone shape. If the hard layer and soft layer are too strongly coupled vertically the exchange spring is too stiff, and the system behaves in the conventional Stoner–Wohlfarth way.

### B. Effect of Lateral Intergranular Exchange Coupling $H_{ex}$

In a second simulation, we keep the value of the vertical coupling constant at  $J = 0.3$  and vary the intergranular exchange  $H_{ex}$ . The vertical branch of the FORC distribution has a prominent peak at positive  $H_b = 2$  kOe, when  $H_{ex} = 1$  kOe [Fig. 3(d)] and becomes more ridge-like with peaks equally distributed between  $H_b = -2$  kOe and  $H_b = +2$  kOe when  $H_{ex} = 4$  kOe [Fig. 3(e)]. If the exchange is increased to  $H_{ex} = 6$  kOe the ridge-like vertical feature splits into two prominent peaks, at  $H_b = \pm 1$  kOe [Fig. 3(f)]. There is an optimum value of exchange for which the FORC distribution has a smooth dependence in  $H_b$ . The FORC distribution also indicates a reduction in media coercivity  $H_c$  with increased exchange. This correlation is associated with the coupled-granular-continuous (CGC) effect [11], [20]. It is clear that the modeled FORC distribution in Fig. 3(e), corresponding to a soft-on-hard structure with  $J = 0.3$  and  $H_{ex} = 4$  kOe, largely reproduces the features of the experimental FORC distribution measured for the multilayer media design in Fig. 2(b).

## V. CONCLUSION

Variations of physical characteristics in the recording media can be conveniently captured by FORC analysis. The FORC diagram for a single-layer granular perpendicular medium has a wishbone shape, well understood within the hysteron model, when a distribution of coercivity values, as well as dipolar interactions are considered. Composite media have a FORC diagram very different qualitatively: the upper branch of the wishbone largely disappears, and the remaining vertical band has a ridge-like structure. This leads us to conclude the vertical interaction between the layers of different  $H_k$  plays a significant role in determining the structure of the FORC distribution. The specific features of this ridge are highly influenced by the intergranular lateral exchange.

## ACKNOWLEDGMENT

The work at the University of California, Davis was supported by the National Science Foundation (NSF) under Grants DMR-1008791, ECCS-0925626, and ECCS-0725902.

## REFERENCES

- [1] A. Berger, Y. Xu, B. Lengsfeld, Y. Ikeda, and E. E. Fullerton, "Delta H(M, Delta M) method for the determination of intrinsic switching field distributions in perpendicular media," *IEEE Trans. Magn.*, vol. 41, no. 10, pp. 3178–3180, Oct. 2005.
- [2] O. Hovorka, Y. Liu, K. A. Dahmen, and A. Berger, "Simultaneous determination of intergranular interactions and intrinsic switching field distributions in magnetic materials," *Appl. Phys. Lett.*, vol. 95, no. 19, p. 192504, 2009.
- [3] A. Berger, N. Supper, Y. Ikeda, B. Lengsfeld, A. Moser, and E. E. Fullerton, "Improved media performance in optimally coupled exchange spring layer media," *Appl. Phys. Lett.*, vol. 93, no. 12, p. 122502, 2008.
- [4] I. D. Mayergoyz, *Mathematical Models of Hysteresis*. New York: Springer-Verlag, 1991.
- [5] C. R. Pike, A. P. Roberts, and K. L. Verosub, "Characterizing interactions in fine magnetic particle systems using first order reversal curves," *J. Appl. Phys.*, vol. 85, no. 9, pp. 6660–6667, May 1, 1999.
- [6] J. E. Davies, O. Hellwig, E. E. Fullerton, G. Denbeaux, J. B. Kortright, and K. Liu, "Magnetization reversal of Co/Pt multilayers: Microscopic origin of high-field magnetic irreversibility," *Phys. Rev. B*, vol. 70, no. 22, p. 224434, Dec. 2004.
- [7] C. R. Pike, C. A. Ross, R. T. Scalettar, and G. Zimanyi, "First-order reversal curve diagram analysis of a perpendicular nickel nanopillar array," *Phys. Rev. B*, vol. 71, no. 13, p. 134407, Apr. 2005.
- [8] M. Winklhofer and G. T. Zimanyi, "Extracting the intrinsic switching field distribution in perpendicular media: A comparative analysis," *J. Appl. Phys.*, vol. 99, no. 8, p. 08e710, Apr. 2006.
- [9] R. K. Dumas, C.-P. Li, I. V. Roshchin, I. K. Schuller, and K. Liu, "Magnetic fingerprints of sub-100 nm Fe dots," *Phys. Rev. B*, vol. 75, p. 134405, 2007.
- [10] G. Choe, J. Park, Y. Ikeda, B. Lengsfeld, T. Olson, K. Z. Zhang, S. Florez, and A. Ghaderi, "Writeability enhancement in perpendicular magnetic multilayered oxide media for high areal density recording," *IEEE Trans. Magn.*, vol. 47, no. 1, pp. 55–62, Jan. 2011.
- [11] T. P. Nolan, B. F. Valcu, and H. J. Richter, "Effect of composite designs on writability and thermal stability of perpendicular recording media," *IEEE Trans. Magn.*, vol. 47, pp. 63–68, Jan. 2011.
- [12] J. W. Liao, R. K. Dumas, H. C. Hou, Y. C. Huang, W. C. Tsai, L. W. Wang, D. S. Wang, M. S. Lin, Y. C. Wu, R. Z. Chen, C. H. Chiu, J. W. Lau, K. Liu, and C. H. Lai, "Simultaneous enhancement of anisotropy and grain isolation in CoPtCr-SiO<sub>2</sub> perpendicular recording media by a MnRu intermediate layer," *Phys. Rev. B*, vol. 82, p. 014423, Jul. 2010.
- [13] R. H. Victora and X. Shen, "Exchange coupled composite media for perpendicular magnetic recording," *IEEE Trans. Magn.*, vol. 41, pp. 2828–2833, 2005.
- [14] A. Y. Dobin and H. J. Richter, "Domain wall assisted magnetic recording," *Appl. Phys. Lett.*, vol. 89, no. 6, p. 062512, Aug. 2006.
- [15] F. Béron, "Propriétés Magnétostatiques de Réseaux de Nanofils via les Courbes de Renversement du Premier Ordre," Ph.D. dissertation, Université de Montréal, Montréal, QC, Canada, 2008.
- [16] X. Kou, X. Fan, R. K. Dumas, Q. Lu, Y. Zhang, H. Zhu, X. Zhang, K. Liu, and J. Q. Xiao, "Memory effect in magnetic nanowire arrays," *Adv. Mater.*, vol. 23, pp. 1393–1397, 2011.
- [17] H. N. Bertram and J. G. Zhu, "Fundamental magnetization processes in thin film recording media," in *Solid State Physics: Advances in Research and Applications*. New York: Academic, 1992, p. 271.
- [18] B. F. Valcu, "Studies in perpendicular magnetic recording," Ph.D. dissertation, Univ. California, San Diego, CA, 2004.
- [19] J. E. Davies, O. Hellwig, E. E. Fullerton, J. S. Jiang, S. D. Bader, Z. T. Zimanyi, and K. Liu, "Crystallinity-dependence of irreversible switching in Fe/SmCo and FeNi/FePt spring magnets," *Appl. Phys. Lett.*, vol. 86, p. 262503, 2005.
- [20] D. Suess, J. Lee, J. Fidler, H. S. Jung, E. M. T. Velu, W. Jiang, S. S. Malhotra, G. Bertero, and T. Schrefl, "Effect of intergranular exchange on the thermal stability and coercive field of perpendicular, single phase, exchange spring, and Coupled Granular Continuous (CGC) perpendicular recording media," *IEEE Trans. Magn.*, vol. 45, pp. 88–99, 2009.